Reverse electrodialysis

Veerman, J.; Saakes, M.; Metz, S. J.; Harmsen, G. J.

Published in:
Journal of Membrane Science

DOI:
10.1016/j.memsci.2008.11.015

Publication date:
2009

Journal of Membrane Science 327 (2009) 136–144

Contents lists available at ScienceDirect

Journal of Membrane Science

journal homepage: www.elsevier.com/locate/memsci

Reverse electrodialysis: Performance of a stack with 50 cells on the mixing of sea and river water

J. Veerman [a], M. Saakes [a], S.J. Metz [a,*], G.J. Harmsen [b]

[a] Wetsus, Centre of Excellence for Sustainable Water Technology, P.O. Box 1113 8900 CC, Leeuwarden, The Netherlands
[b] State University Groningen, Nijenborg 4, 9747 AG Groningen, The Netherlands

ARTICLE INFO

Article history:
Received 15 July 2008
Received in revised form
26 September 2008
Accepted 9 November 2008
Available online 18 November 2008

Keywords:
Reverse electrodialysis
Inverse electrodialysis
Salinity power
Salinity gradient power
Power density
Energy efficiency
Power production

ABSTRACT

The purpose of reverse electrodialysis (RED) is to produce electricity upon the mixing of two solutions. We studied the power density (W/m^2) and the energy efficiency (the amount of energy produced from specified volumes of river and sea water in relation to the thermodynamic maximum). With a stack of 50 cells (of 10 cm × 10 cm), a power density of 0.93 W/m^2 was obtained with artificial river water (1 g NaCl/L) and artificial sea water (30 g NaCl/L), which is the highest practical value reported for RED. This value is achieved due to an optimized cell design using a systematic measurement protocol.

The main factor in the power density is the cell resistance. With the used membranes (Fumasep FAD and FKD) and a spacer thickness of 200 μm, a cell resistance of 0.345 Ω is measured under RED conditions. This is about one and a half times the value as expected from the contribution of the individual components. This high value is probably caused by the shielding effect of the spacers. The largest contribution to this resistance (about 45%) is from the river water compartment.

The hydrodynamic loss resulted in a maximal net power density of about 0.8 W/m^2 at a flow rate of 400 mL/min. At this optimum the consumed power for pumping is 25% of the total generated energy. The majority of the pump power is lost in the manifolds.

Multistage experiments were performed at maximal power conditions (a current density of about −30 A/m^2 and at a flow rate of 300 mL/min). At these conditions the theoretical energy efficiency is maximal 50%. In practice however, the energy efficiency of a single stack is 9%. The effluent concentrations of the so operated stack are used for a second experiment and so on, simulating a multistage operation. With 3 stages a cumulative energy efficiency of 18% is achieved. A fourth stage did not increase this value. The power density of the 3 stages together was 50% of the power density of the first stage, indicating that energy efficiency and power density are counteracting.

Further increase of power density and energy efficiency can be obtained with a better spacer and manifold design. A more open spacer is beneficial for RED in two ways: less shielding and lower pressure drop. Less shielding decreases the electrical resistance of the cell. A lower pressure drop permits the use of thinner water compartments, resulting again in a decreased electrical resistance of the cell and an improvement of the power density.

1. Introduction

In 1954 Pattle [1] wrote: *The osmotic pressure of sea-water is about 20 atmospheres, so that when a river mixes with the sea, free energy equal to that obtainable from a waterfall 680 ft high is lost. There thus exists an untapped source of power which has (so far as I know) been unmentioned in the literature.* This 'salinity power' is in principle clean and sustainable and gives no thermal pollution and no CO_2 exhaust. The energy that theoretically can be generated per m^3 river water is 2.5 MJ when mixed with a large surplus of sea water or 1.7 MJ when mixed with 1 m^3 sea water (Table 1). Wick and Schmitt [2] estimated the total global salinity power to be 2.6 TW, which is sufficient to supply the global electricity demand (2 TW) or 16% of the total present energy consumption [3]. There are different methods to extract energy from the mixing of sea and river water. Described techniques are reverse electrodialysis (RED) [1,4,5], pressure retarded osmosis (PRO) [6,7], vapor pressure difference utilization [8], mechanochemical methods [9], the so called 'hydrocratic generators' [10], membrane-less hydro-voltaic cells [11] and cryoscopic techniques like freezing temperature difference utilization [12]. RED as well as PRO are promising techniques for the generation of energy from a salinity gradient. Post et al. [13]

* Corresponding author. Tel.: +31 58 284 62 00.
E-mail address: sybrand.metz@wetsus.nl (S.J. Metz).

0376-7388/$ – see front matter © 2008 Elsevier B.V. All rights reserved.
doi:10.1016/j.memsci.2008.11.015

Table 1
Gibbs free energy from mixing V_R (m^3) river water (S_R = 0 kg NaCl/m^3) with V_S (m^3) sea water (S_S = 30 kg/m^3) at 298 K.

V_R (m^3)	V_S (m^3)	V_R/V_S	ΔG_{RED} (MJ)
∞	1	∞	∞
10	1	10	6.1
2	1	2	2.8
1	1	1	1.76
1.26	*0.74*	*1.72*	*1.87*
1	2	0.5	2.06
1	10	0.1	2.43
1	∞	0	2.55

showed that in the case of sea water with river water, RED is very promising.

In principle, RED is a seemingly simple technique. Nevertheless, only 8 groups have published in scientific journals on their experimental results with RED operating on sea and river water [1,4,5,12,14–20] during a period encompassing more than 50 years. In these papers RED has been proven on lab scale. However, the reported power densities were relatively low and the efficiency of the process (energy efficiency) was not taken into account. Meanwhile, the knowledge of ion exchange membranes has increased and many ion exchange membranes with good properties have been developed. Furthermore, energy demand, and therewith also the problems concerning chemical and thermal pollution as well as greenhouse problems caused by CO_2 exhaust, has grown enormously. The investigation of this technique using state of the art membranes and the improvement of the operational properties of the process is aimed at providing a solution to these problems.

The objective was to study the behavior of a RED stack with commercially available membranes with respect to two operational important parameters: energy efficiency (the gained power in relation to maximal thermodynamic value) and power density (the power generated per m^2 membrane). These two response factors are dependent on membrane properties (conductivity, selectivity, osmotic behavior), cell properties (compartment thickness, spacer type), stack design parameters (way of feed, electrode system), operating conditions (flow rates, electrical load) and water quality (salt content, impurities, temperature, polyvalent ions). These parameters are conflicting in many ways. This article focuses on the main parameters affecting power density and energy efficiency: (i) current density, (ii) membrane and spacer resistance, and (iii) feed flow rate. In order to obtain a maximal power density we used commercial membranes with a low resistance. Experiments were performed with a custom made RED stack with a variable number of cells. The largest stack consisted of 50 cells with a total effective membrane area of 1 m^2, generating a power output of 0.93 W which is the highest power density ever reported for RED operating on river and sea water.

2. Theory

2.1. Reverse electrodialysis

A typical RED system consists of a variable number of alternating cation and anion exchange membranes in a stack. Fig. 1 shows such a system with only one cell. Every cell consists of a cation exchange membrane (CEM), a salt water compartment, an anion exchange membrane (AEM) and a sweet water compartment. Positive ions from the sea water diffuse through the CEMs to the river water compartment and build up a positive potential on one side of the stack. The negative ions from the sea water diffuse through the AEMs to the river water compartment on the other side and cause a negative potential in this location. The potential difference between the two solutions can be calculated using the Nernst equation. If sea water is considered as a solution of 30 kg NaCl/m^3 and river water as a solution of 1 kg NaCl/m^3, this potential difference is 140–160 mV per cell. If there is an external circuit connected to the end electrodes, electrical power can be extracted from the system. The ionic current in the cells is then converted to an external electron current via redox reactions at the electrodes.

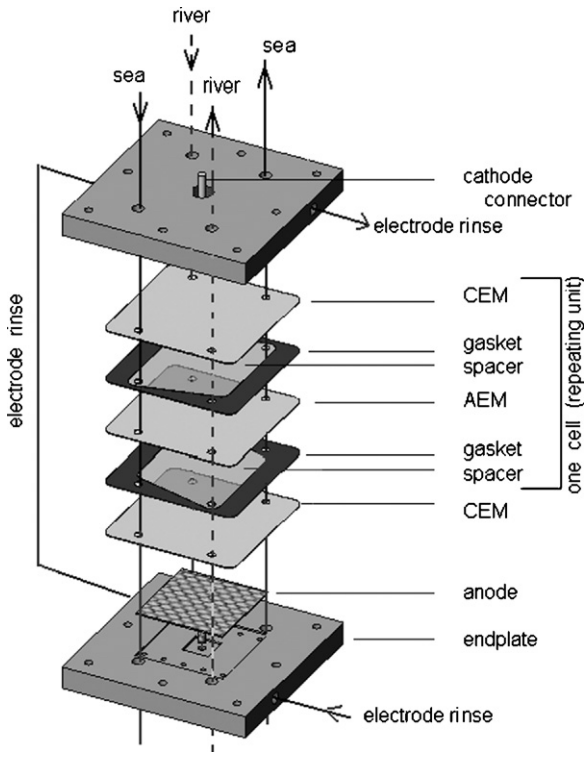

Fig. 1. A reverse electrodialysis stack with one cell.

2.2. Power density determination

The theory about reverse electrodialysis was formulated by Weinstein and Leitz [14], Clampitt and Kiviat [21], Jagur-Grodzinski, and Kramer [17] and Lacey [22] and is summarized by Veerman et al. [20]. Key parameters of a RED cell are the electromotive force, internal resistance and delivered power. The voltage across a 100% selective membrane can be calculated if pure NaCl solutions of 1 and 30 g/L at 298 K are used, giving values of 0.080 V for a CEM and 0.078 V for an AEM, or together E_{cell} = 0.158 V for a cell.

The power efficiency (η_P) is the fraction of total power that is delivered to an external power consumer with resistance R_u:

$$\eta_P = \frac{I^2 R_u}{I^2 R_i + I^2 R_u} = \frac{R_u}{R_i + R_u} \quad (1)$$

At the condition of maximal power output ($R_u = R_i$), the power efficiency is not higher than 50%. A higher efficiency can be achieved (by taking $R_u > R_i$) at the cost of a decreased power output.

The power density P_d of a RED system is defined as the external power per membrane area (W/m^2) and is maximal under the condition of $R_u = R_i$:

$$P_d = \frac{P_u}{2A} = \frac{I^2 R_u}{2A} = \left(\frac{E_{cell}}{R_i + R_u}\right)^2 \frac{R_u}{2A}$$

$$= \frac{E_{cell}^2}{8AR_i} = \frac{E_{cell}^2}{8A(R_{AEM} + R_{CEM} + R_{river} + R_{sea})} \quad (2)$$

where A stands for the active cell area and $2A$ for the total membrane area (AEM and CEM) in a cell. R_{AEM}, R_{CEM}, R_{river} and R_{sea} are

the resistances of the AEM, CEM, river water compartment and sea water compartment, respectively.

2.3. The mixing entropy of sea water and river water

In order to determine the amount of energy extracted from mixing, it is necessary to calculate the chemical potential between 2 solutions of different concentrations. The Gibbs free energy of mixing (ΔG_{RED}) of river water (V_R (m^3); NaCl concentration: C_R (mol/m^3)) with sea water (V_S (m^3); NaCl concentration: C_S (mol/m^3)) is given by [23,24]:

$$\Delta G_{RED} = 2RT \left[V_R C_R \ln \frac{C_R}{C_M} + V_S C_S \ln \frac{C_S}{C_M} \right] \quad (3)$$

with

$$C_M = \frac{V_R C_R + V_S C_S}{V_R + V_S} \quad (4)$$

where R is the gas constant ($R = 8.31432\ J\ mol^{-1}\ K^{-1}$) and T the temperature (K); the origin of the factor 2 is the dissociation of one mole NaCl in two moles of ions. C_M is the equilibrium concentration, gained at total mixing. Eq. (3) is an approximation: the entropy increase of the water is not included and the activity coefficients are taken to unity but both effects tend to counterbalance.

For a zero salt concentration in the river water ($C_R = 0$), Eq. (3) can be simplified to

$$\Delta G_{RED}\ (C_R = 0) = 2RT \left[V_S C_S \ln \frac{V_S + V_R}{V_R} \right] \quad (5)$$

In an ideal RED process, all the Gibbs free energy is liberated as electrical energy. Table 1 shows this amount of energy produced for different mixing ratios of sea water (30 kg NaCl/m^3) and river water (0 kg NaCl/m^3) at 298 K. With 1 m^3 sea water and 1 m^3 of river water 1.76 MJ can theoretically be generated. With a large surplus of sea water this value is 2.55 MJ. Table 1 also shows that in cases where the amount of salt water is the limiting factor, using an excess of salt water is very useful (compare the 6.1 MJ of the V_R:V_S = 10:1 combination with the 2.42 MJ for V_R:V_S = 10:1). Such cases may be industrial processes with a brine effluent together with river or sea water.

In case of river water used with sea water, Eq. (3) suggests the use of a surplus of sea water. However, the costs of pretreatment, transport and pumping through the stack should also be taken in account from an economical viewpoint. Assuming these costs are equal per m^3 for each type of water, the optimal ratio V_S/V_R can be obtained by substituting $V_R = 1$ in Eq. (3) and subsequently differentiating the equation with respect to V_S. Solving $d(\Delta G_{RED})/d(V_S) = 0$ gives $V_R/V_S = e - 1 \approx 1.72$. This ratio results in a slightly higher energy compared to the 1:1 mixture with the same total volume of 2 m^3 as shown in Table 1 (in italics).

By substituting the flows rates Φ for volumes V, Eq. (3) can used for calculating the free Gibbs energy per second before and after mixing in the RED stack:

$$X = 2RT \left[\Phi_R C_R \ln \frac{C_R}{C_M} + \Phi_S C_S \ln \frac{C_S}{C_M} \right] \quad (6)$$

The equilibrium concentration C_M can be obtained with Eq. (4) by using flow rates instead of volumes.

The available free energy is also called 'exergy'. The consumed free energy per second for the RED installation is obtained by taking the difference of output and input free energy per second:

$$X_{cons} = X_{out} - X_{in} \quad (7)$$

3. Experimental

The RED cell which was used in our experiments is shown in Fig. 1. The specific components are described in the following sections.

3.1. Endplates

Electrode compartments are situated inside the endplates. Endplates were milled from reinforced phenol formaldehyde (Epratex HGW 2082, Eriks, The Netherlands). Stainless steel bolts were used to close the stack. The distance between the end plates was about 33 mm in the case of 50 cells with 200 μm spacers and 200 μm gaskets.

3.2. Cells

The functional area of one membrane was 100 cm^2. On the outsides of the stacks cation exchange membranes were used as shielding membranes to prevent the transportation of negatively charged iron complexes. Fumasep anion and cation exchange membranes FAD and FKD with a thickness of 0.082 mm (obtained from Fumatech, Germany) were used. The stacks were equipped with polyamide woven spacers with a thickness of 200 μm. The membranes, gaskets and spacers were made at their correct size by means of a punch and a press.

3.3. Electrode system

The electrode compartments contained a solution of NaCl (1 mol/L) with $K_4Fe(CN)_6$ (0.05 mol/L) and $K_3Fe(CN)_6$ (0.05 mol/L). This electrolyte was pumped through the anode and cathode compartment at a rate of 60 mL/min. All chemicals used were technical grade and purchased from Boom, Meppel, The Netherlands. Titanium mesh end electrodes, coated with Ru–Ir mixed metal oxides with dimensions of 10 cm × 10 cm were used (Magneto Special Anodes b.v., Schiedam, The Netherlands). These electrodes are suitable as anode as well as cathode and therefore current reversal is possible.

3.4. Sea and river water

Demineralized water with technical grade sodium chloride (Boom, Meppel) was used. 'Sea water' consisted of 30 g NaCl/L and 'river water' of 1 g NaCl/L. A conduction meter with a Tetracon 325 cell (WTW, Weilheim, Germany) was used. To convert conductivities to salt content, a second-order calibration line was made in the 0–30 kg NaCl/m^3 range at 298 K. Peristaltic pumps (Masterflex L/S, Cole Parmer Instrument Company) were used for the delivery sea and river water and for recirculation of the electrode rinse. The stack with 50 cells was fed with 700 mL/min. Smaller stacks were fed with proportional lower flow rates, thereby maintaining the same flow velocity along the membrane surface. The temperature was controlled at 298 ± 1 K for all experiments.

3.5. Reference electrodes

Platinum electrodes (diameter 1 mm) were inserted near the centre of the working and counter electrode through the meshes of the electrode grid and adjusted until the end was in plane with the inner surface of the end electrode. The Pt-wire was covered with epoxy and the end was scoured and polished afterwards. The measuring system based on Pt-electrodes was compared with a system of Ag/AgCl reference electrodes and showed the same results.

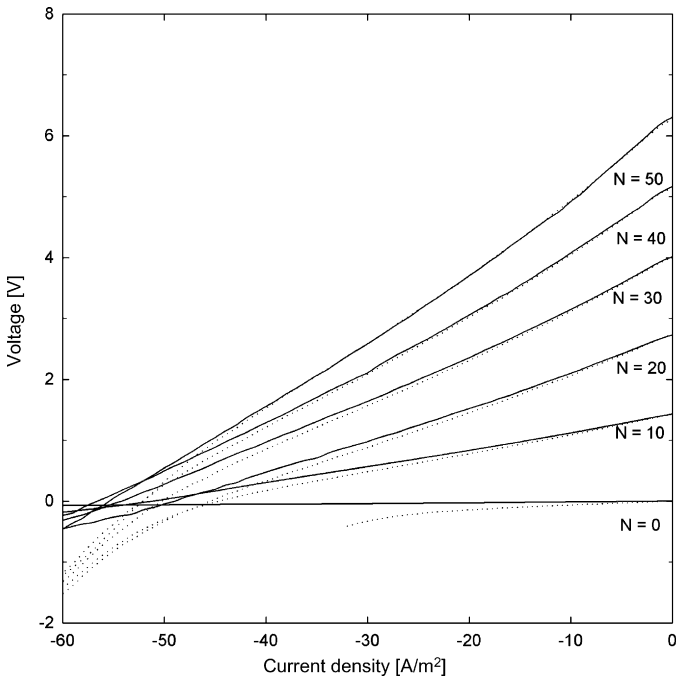

Fig. 2. *EJ*-curve curves for a stack with 0, 10 . . . 50 cells. Each curve is measured on the reference electrodes (solid lines) and on the end electrodes (dashed lines).

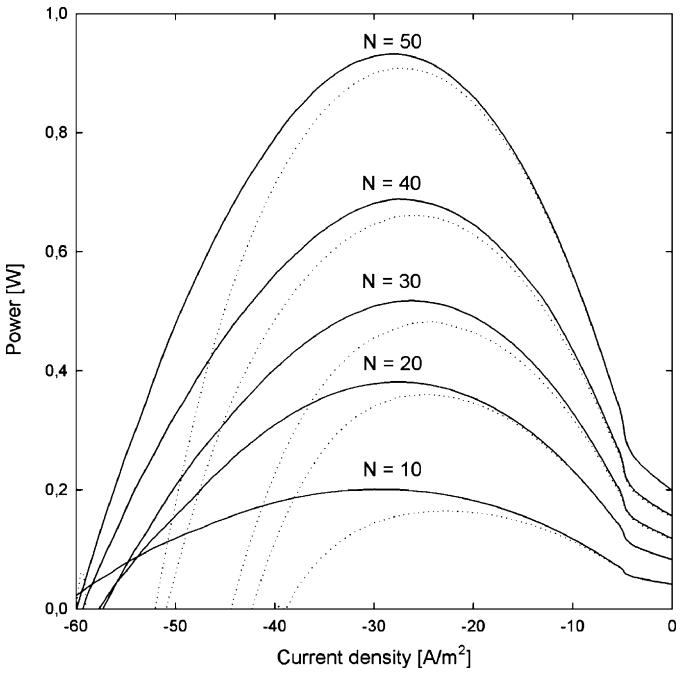

Fig. 3. Measured power of stacks with 0, 10 . . . 50 cells. The solid line is the power generated by the stack and the dashed line is the output on the work electrodes.

3.6. Electrical measurements

The measurements were carried out with an Ivium potentiostat (Ivium Technologies, Eindhoven, The Netherlands) in the galvanostatic mode. The galvanostatic scan rate was always set to 2 mA/s. Initially, the voltage (E) as function of the electrical current (I) was measured, resulting in an *EI*-plot. In most graphs in this paper, the electrical current is transformed to the current density (J) and galvanostatic scans appear as *EJ*-curves.

4. Results and discussion

4.1. Variable cell number experiments

In order to determine the maximum power output of a RED stack, the stack voltage as function of the current density was measured. The applied current was controlled via a potentiostat. The optimal load (the external electrical resistance) for a maximal power density was determined with these values. The power output is maximal when the load equals the internal resistance Eq. (1). *EJ*-curves plotted of a full stack with 50 cells, with 40 cells and so on (N = 50, 40, 30, 20, 10 and 0) are shown in Fig. 2. A stack with 0 cells contained only 1 CEM between the electrode compartments. The voltage at the end electrodes (the working and the counter electrode) is represented by the dashed lines, the voltage on the reference electrodes by solid lines. At zero current density, both voltages are equal; at lower current densities the voltage on the end electrodes is slightly lower due to overpotentials at the electrode and a voltage drop inside the electrode compartment.

Fig. 3 shows the power as function of the current density derived from Fig. 2 for different stacks (the solid lines). This power is determined from the potential measured at the reference electrodes multiplied by the current density throughout the stack. The potential measurement on the reference electrodes does not contain energy loss due to redox processes at the electrode. Therefore, this value gives the actual power obtained from the mixing of sea and river water via the RED stack. The 50 cell stack contains a total membrane area of 1 m^2 and therefore also represents the power density; the maximal (0.93 W/m^2) is reached at a current density of −28 A/m^2. At this point the theoretical energy efficiency is not more than 50%. Between 0 and −28 A/m^2, the energy efficiency is higher but the power density is lower. The obtained power density (0.93 W/m^2) is substantially higher than the power densities for the river water/sea water RED system published so far (Table 2). Furthermore, it can be observed from Fig. 3 that the power increases almost linearly with the number of cells (N = 10: P = 0.20 W; N = 20: P = 0.40 W; . . . ; N = 50: P = 0.93 W). This indicates that the loss due to leaking currents is minimal [20]. The differences between the solid and the dashed lines represent the loss due to electrode reactions and an Ohmic drop in the electrode compartments. This loss is relatively low for large stacks as is shown by the experiment with the 50 cells.

4.2. Factors affecting the cell resistance

Central in the considerations about power density is the cell resistance, the denominator in Eq. (2). The cell resistance should be minimal in order to obtain a maximal power output. The resistance of a RED stack can theoretically be determined by the addition of the resistances of the individual components: the resistances of an AEM, a CEM, a river water compartment and a sea water compartment. Membrane resistances are tabulated normally for 0.5 M NaCl

Table 2
Reported power density P_d (W/m^2) and spacer thickness δ_M (mm) with solutions of 1 and 30 g NaCl/L by different authors.

Author	Year	Power density (W/m^2)	Membrane thickness (mm)
Pattle [4]	1955	0.05	0.7
Weinstein and Leitz [14]	1976	0.17	1
Audinos [15]	1983	0.40[a]	3
Jagur-Grodzinski and Kramer [17]	1986	0.41	0.55
Turek [18]	2007	0.46	0.19
Suda [19]	2007	0.26	1
Veerman et al. [20]	2008	0.95	0.2

[a] With 'sea' of 295 g/L.

Table 3
Experimental area resistances of FAD and FKD ion-exchange membranes. The resistances between sea and river water (in italics) are calculated.

Salt content (kg/m^3)		Area resistance (Ω cm^2)	
A	*B*	FAD	FKD
30	30	0.88	3.75
1	1	11.5	44.7
1	30	*1.63*	*5.9*

conditions which is comparable to the sea water concentration. It is proven that the membrane resistance depends on concentration [25,26]. Measurements by Długołęcki et al. [27] show this concentration effect for the membranes used in the experiments described in this paper (Table 3). The values determined by Długołęcki are obtained for equal concentrations on both sides of the membrane. However, in the case of RED, there exists a concentration profile over the membrane. An estimation of the membrane resistance during RED operation is made by fitting the membrane resistance as a function of concentration and integrating this over the whole membrane thickness (Appendix A). It follows that the estimated membrane resistance under RED conditions (between NaCl solutions of 30 and 1 g/L) is about twice the resistance under normal membrane test conditions (between identical NaCl solutions of 30 g/L).

If the sea and river water compartments did not contain any spacer, 'spacer-less resistances' of these compartments could be established from the dimensions of the compartment and the specific resistance of the concerning salt solution. However, spacers inhibit the ion flow. The woven spacers used in the experiments described in this paper occupy 33% of the volume and 49% of the area in a plane projection, resulting in obstruction factors f for the ionic current of $1/(1-0.33)=1.49$ or $1/(0.49)=1.96$. The first value is an underestimation because the ionic current follows a tortuous path between the threads of the spacer. The second value is an overestimation because the current can follow curved paths. Therefore, for the calculation of cell resistance all 'spacer-less resistances' were multiplied with obstruction factor f (the average of both values: $f=1.72$). The calculated and measured resistances of a single cell (10 cm $\times$ 10 cm; spacers of 200 μm) are shown in Table 4. The table shows the resistance for the case where both compartments are fed with sea water (SS), both with river water (RR) and with sea and river water (SR). From Table 4, it follows that under normal RED operation (column SR), the river water compartment has the largest contribution to the total resistance.

These theoretical values were compared with the experimental data which were determined for 3 different cases when the different compartments are filled with (i) both with sea water, (ii) both with river water and (iii) one with sea water and the other with river water (the normal RED operation) (Fig. 4). The current density is varied from -60 to 0 A/m^2 in order to determine the cell resistance from the slope of the *EJ*-curves. As shown in Fig. 4,

Table 4
Calculated and measured resistance and power density of a cell ($A=0.01$ m^2) with Fumasep membranes (FAD and FKD). The cell is fed with sea and river water (SR, left column), with sea and sea water (SS, middle column) and with river water with river water (RR, right column).

	Feed	SR	SS	RR
Calculated	FAD (Ω)	0.016	0.009	0.115
	FKD (Ω)	0.059	0.038	0.447
	Sea water comp. (Ω)	0.007	0.007	0.155
	River water comp. (Ω)	0.156	0.007	0.155
	Cell resistance (Ω)	0.238	0.061	0.872
	Power density (W/m^2)	1.18	–	–
Experimental	Cell resistance (Ω)	0.345	0.067	0.734
	Power density (W/m^2)	0.93		

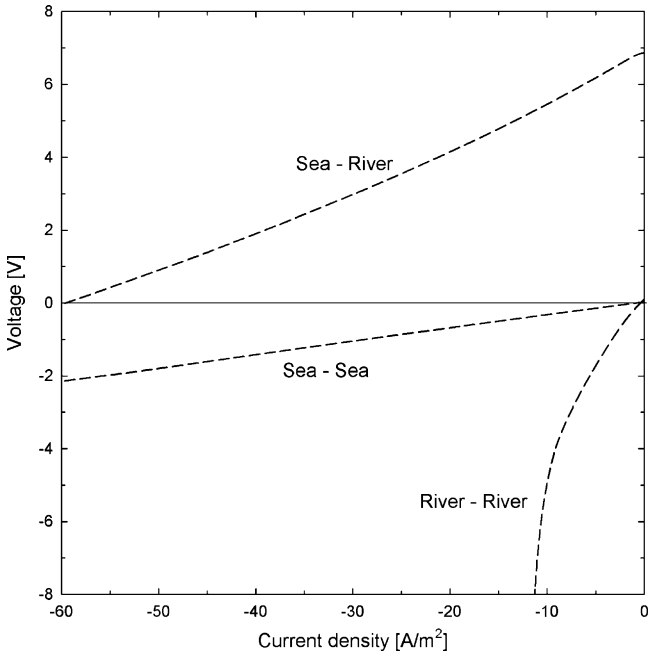

Fig. 4. *EJ*-curves at the Pt-reference electrodes for a stack with 50 cells: (a) normal, (b) sea–sea and (c) river–river.

there is no potential difference for sea/sea and river/river at zero current density. In fact, the operation mode here is not RED but normal ED resulting in a salt depletion in one compartment and an enrichment in the other. In the river/river case, this disproportion of the salt concentration causes an extremely high resistance and sharply curved lines at higher (negative) current. In the normal RED operation (sea/river) the opposite effect occurs: at a high negative current there is a NaCl transport from the sea water to the river water compartments resulting in a lower resistance at increased negative current.

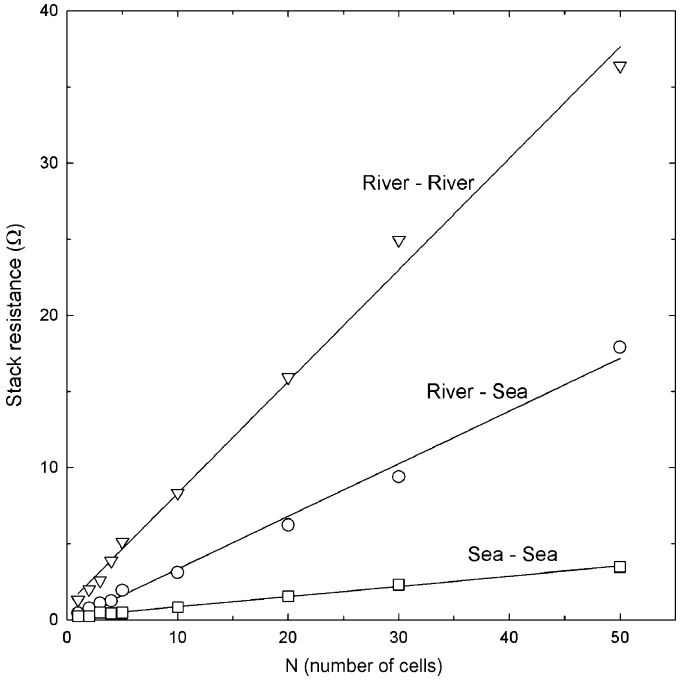

Fig. 5. Stack resistance of stacks with different number of cells.

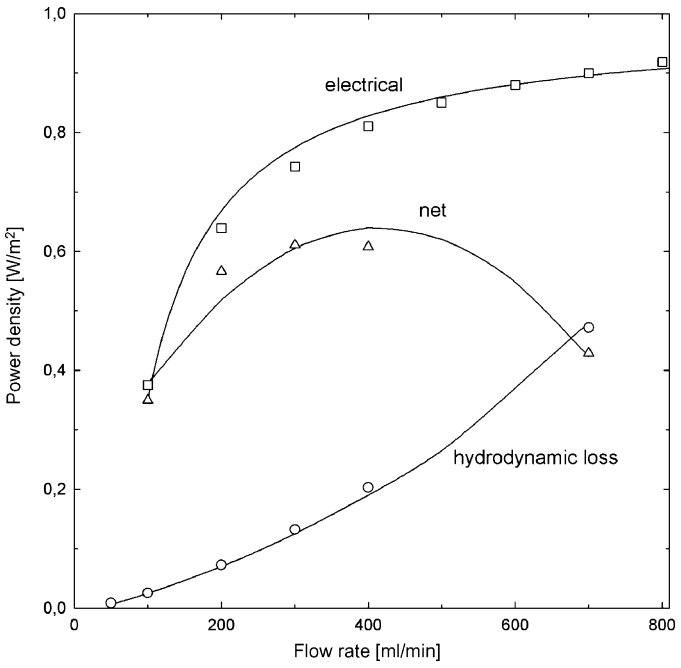

Fig. 6. Generated electrical power, hydrodynamic loss and the supplied net power in a 50 cell stack.

From these *EJ*-curves the cell resistance can be obtained at different current densities. The experiment is done with a cell of 50, 30, 20, . . . , 1 cell. The results are presented in Fig. 5. The resistances were calculated near $J = 0$ by calculating $\Delta E/\Delta I$ over the range −50 to 0 mA of the scan. The single cell resistance is the slope of the different lines and is 0.73 Ω for the river/river system, 0.35 Ω for the sea/river system (normal RED) and 0.067 Ω for the sea/sea system and tabulated in Table 4.

In Table 4 the calculated power density (1.18 W/m^2) has been added according Eq. (2); for the cell voltage E_{cell} is taken the value of 0.150 V, based on a permselectivity of both membranes of 0.95 and on an ideal cell voltage of 0.158 V [20]. Measured power density (0.93 W/m^2) is 21% less than the calculated value, which is close to the theoretical values if the obstruction of the spacer is taken into account. If no spacer would be used and the compartment thickness would be unaffected, a theoretical value of 1.65 W/m^2 is possible. This shows that further improvement of the power density of RED is obtainable with a more open spacer material or no spacer at all. Długołęcki et al. [27] presented a power density model dependent on spacer thickness and area resistance and permselectivity of the membranes. With the best available commercial membranes and spacers of 150 μm, they estimated a power density of about 5 W/m^2.

4.3. Effect of the flow rate on the power density

The net power output (P_u) is determined by subtracting the hydrodynamic loss from the produced power output. Fig. 6 shows the results in the range 200–1000 mL/min together with their difference, the net power. High flow rates of sea and river water maintain high concentration differences across the membranes and reduce concentration polarization. On the other hand, high flow rates cause higher pressure losses and lower the net power output. There exists an optimal flow regime for a given cell configuration, where the net power output is maximal. In Fig. 6 the electrical power P_u is fitted to the flow rate (Φ) by the following function (d and e are fit variables).

$$P_u = d - \frac{e}{\Phi} \tag{8}$$

The hydrodynamic power losses are fitted by a parabolic function:

$$P_{pump} = a\Phi^2 + b\Phi + c \tag{9}$$

where a, b and c are specific constants for the system. The maximal net electrical power is reached near 400 mL/min (0.7 cm/s). At this optimum the consumed power for pumping is 25% of the total generated electrical energy. The hydrodynamic loss is relatively high in these experiments where the pressure was measured outside the stack. Experiments with pressure measurements in the spacer compartments show a much lower pressure drop [28]. The residual pressure losses are caused by the internal manifolds. Experiments with pressure measurements within cells showed pressure losses in the manifolds of 80% of the total pressure drop over the whole cell. The design of the manifolds is very critical and these locations are subject to obstruction by pollution and mechanical deformation of the stack. Besides improving the manifolds, the pressure drop can be decreased by using more open spacer material. Another approach is the use of relatively thick sea water spacers: if they are five times thicker than the river water spacers, then the fluid resistance and the electric resistance are negligible compared to the river water compartment. However, the resulting decrease in lateral electrical resistance that causes an increased ionic shortcut current is a point of attention [20].

4.4. Cascade operation

Multistage RED experiments were performed as shown in Fig. 7. Instead of using 4 separate RED stacks in series as Fig. 1 suggests, experiments were done with only one RED stack, each time operating with inlet concentrations equal to effluent concentrations of the preceding experiment. This way a four 4 stage operation was simulated. The first stack was fed with solutions of 0.34 g/L (river water) and 30.8 g/L (sea water), both with a flow rate of 300 mL/min. All stacks were operated with the same electrical current of −300 mA

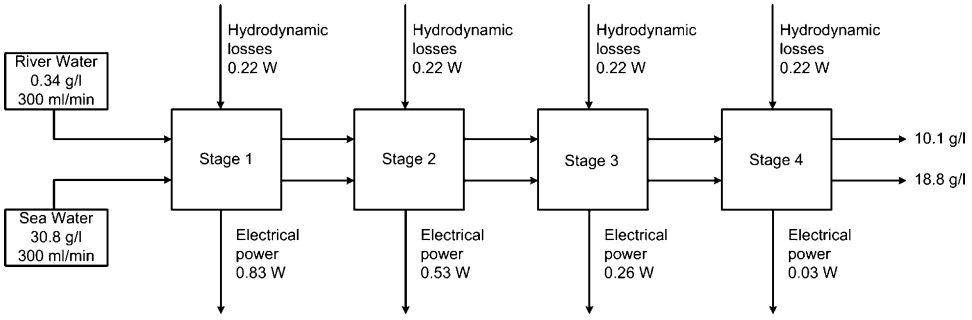

Fig. 7. In- and out-going potential salinity power, the delivered electric power and the hydrodynamic losses in a four stage experiment with a 50 cell stack with a total membrane area of 1 m^2.

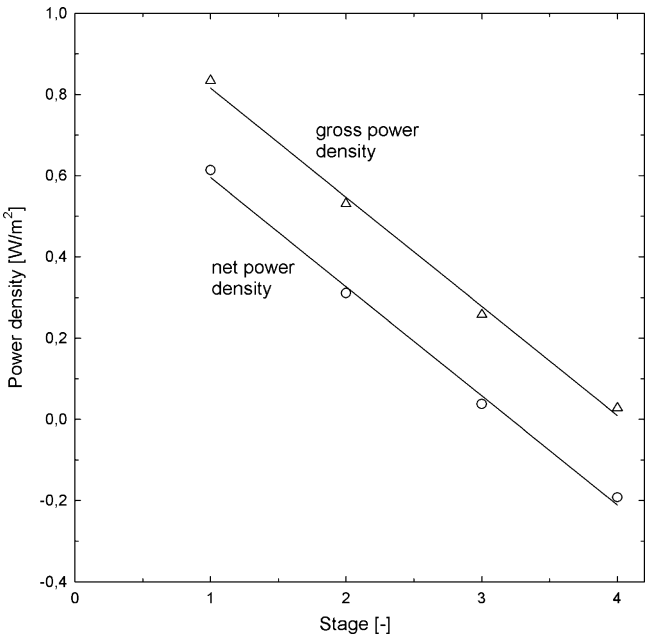

Fig. 8. Power density and the hydraulic loss for each stage at a four stage experiment in a 50 cell stack with a total membrane area of 1 m^2.

to simulate a real serial operation of the four stages. Determined at this current were (i) the salt concentrations of the in and outgoing streams (from the conductivity), (ii) the water flow rates, (iii) the pressure drop between outlet and inlet of the stack, (iv) the ingoing water temperatures, (v) the potential salinity power from mixing as calculated from Eqs. (6) and (7), (vi) the delivered electrical power (from the voltage at the reference electrodes) and (vii) the hydraulic loss (from the flow and pressure drop).

In each stage, the electricity was generated near maximal power conditions (the external electrical resistance is equal to the internal resistance) with the consequence that 50% of the potential salinity power is lost in any case. Another part of the salinity power is lost by NaCl transportation and osmosis through the membranes, by ionic shortcut currents [20] and by irreversible mixing due to internal leakage in the stack.

The generated electrical power density (gross power) and the net electrical power (gross power minus pressure losses) from each stage in Fig. 7 are plotted in Fig. 8.

The gross energy efficiency is defined as follows:

$$Y_{\text{gross}} = \frac{P_{\text{u}}}{X_{\text{max}}} \tag{10}$$

with P_{u} the generated (and usable) electric power. The flow ratio (the sea water flow divided by the river water flow) and a possible addition of NaCl to the river water are not prescribed.

In the net energy efficiency Y_{net}, a correction for the hydrodynamic loss is made as well:

$$Y_{\text{net}} = \frac{P_{\text{u}} - P_{\text{pump}}}{X_{\text{max}}} \tag{11}$$

Fig. 8 indicates that only two stages are useful. However, in the case of a large reduction of the hydraulic losses, the third stage can also contribute to the net energy yield. In this scheme the electrical power consumed by the electrode system is not included. This dissipated power is about 10% of the generated electrical power for a stack with 50 cells and is marginal in large stacks.

Fig. 9 shows the effect of multiple stages on the cumulative gross power density and the cumulative gross energy efficiency: it follows that both important RED parameters are counteracting. However, these values depend on the mode of operation (current density) and the stack design (pressure drop).

The most important response variables of a RED stack are the power density P_{d} and the net energy efficiency $Y_{\text{net.}}$ A commercial RED installation should operate at high power generation and low water consumption. These requirements are conflicting in many ways. A high power density is preferred when the equipment costs are the main costs and there is an excess of river water. However, when the pretreatment costs of water are substantial or the amount of river water is limited, it may be interesting to operate at a lower power density, thereby increasing the energy efficiency. There are many factors that influence both goals, such as flow rates, spacer thickness, stack design, river water concentration, current density, and so on. Maximizing the power of a special installation gives well-defined values of different parameters; minimizing the fuel (water) consumption requires low flow rates and a high external load while the power output is relatively low.

4.5. Comparison of RED and ED

The most important difference between RED and ED (as used for desalination) are the products: electrical power and drinking water. The market price of these products dictate in general the design differences between the techniques and to a less order the requirements of the product and operational differences.

Table 1 shows the generated amount of energy for different mixing ratios: for the most realistic 1:1 ratio there can be generated a theoretical maximum of 1.7 MW. In relation to fossil fuels this is a very low energy density. To operate on an economical base, high power densities and high energy efficiencies should be achieved. This requires a very sophisticated design with tuned operational variables. These are low electrical resistance (thin compartments, thin membranes), low fluid resistance (well designed spacers and manifolds), high energy efficiency (high permselective membranes), a high degree of exhaustion of the feed water (multistage operation), and an efficient electrode system. At this moment there are not yet special membranes and spacers for RED.

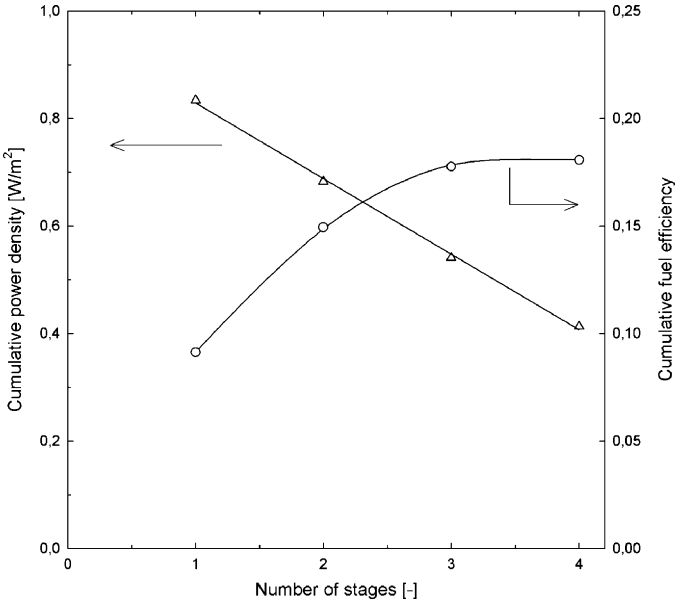

Fig. 9. Cumulative power density and cumulative gross energy efficiency of a system with 1, 2, 3 and 4 stages.

In contrast the suitability of the ED technique is dictated by the water price and by product requirements. Energy consumption is a second interest. For making drinking water, all materials should satisfy to food quality regulations. This concerns pumps, piping, spacers and especially the membranes. This is only possible with a rather robust and over dimensioned structure.

5. Conclusions

In this paper we show that the actual power density of a RED stack operated on artificial sea and river water is 0.93 W/m^2, which is the highest reported value for a real stack operation. This value is obtained with low resistance membranes, good sealing of the compartments, with small compartment thickness (200 μm) and an accurate method to determine the stack performance. 25% of this produced power is lost by pressure drop by using commercially available spacers. We show that this pressure drop is mainly caused by the resistance of the manifolds. The net produced power also depends on the flow rate. At high flow rates, it increases due to reduced concentration polarization, and decreases due to higher pressure losses. The optimal value is found at 400 mL/min. The total cell resistance is one and a half times higher as expected from the contribution of the individual components. This may be caused by the shielding effect of the spacer. A more open spacer is beneficial for RED in 2 ways: less shielding and lower pressure drop. The membrane resistance is of minor importance in the tested stacks, because the 200 μm river water compartment has a dominant influence on the total cell resistance. The energy efficiency of 4 cells which are operated in series is also shown. A gross energy efficiency of 18% is achieved in a 4 stage operation at maximal produced power. This value was achieved under conditions of maximal power density were the maximal energy efficiency is 50%. The results are encouraging for further efforts on the improvement of the system.

6. Recommendations

Power density and energy efficiency are counteracting. Nowadays there is plenty of unused fuel (river water) and a RED installation is at present rather expensive. The first goal is to increase the power density, but proving the possibility of a high energy efficiency is likewise necessary in order to make reverse electrodialysis a substantial energy source in the future.

The described results are encouraging and are the basis of further investigations. The central theme will be describing the power density and the fuel efficiency in terms of membrane and spacer properties, stack and cell dimensions, fluid velocities and so on. Furthermore, the search for improved membranes, spacers, gaskets and electrode systems is ongoing. Also the use of real sea and river water in RED and its effect on the performance fouling, spacers and membranes needs to be investigated. Fouling should be prevented by a balanced basic pre-treatment and improved, very open spacers. The goal is an economical performing RED installation operating on river water and sea water.

Acknowledgements

This research was performed at Wetsus, centre of excellence for sustainable water technology. Wetsus is funded by the city of Leeuwarden, the province of Fryslân, the European Union European Regional Development Fund and by the EZ/Kompas program of the Samenwerkingsverband Noord-Nederland. The first author would like to thank the Noordelijke Hogeschool Leeuwarden who facilitated this research by detaching him to Wetsus and the participants of the energy theme for their interest and financial contribution.

Appendix A. Resistance of a membrane between two solutions with different concentration

Długołęcki et al. [27] have measured the area resistance of FKD and FAD membranes at different NaCl concentrations. We fitted exponential functions to these data points:

$$R_{\text{area}}(C) = p + qe^{-rC} \tag{12}$$

where R_{area} is the area resistance of the membrane, C the concentration and p, q and r fit parameters.

Fitting resulted in $R_{\text{area}} = 4.37 + 99.4e^{-53.1C}$ for the FKD and $R_{\text{area}} = 0.91 + 17.6e^{-29.8C}$ for the FAD membrane. The effective area resistance R_{eff} can be determined by integrating the exponential function between the concentration boundaries C_1 and C_2.

$$R_{\text{eff}} = \frac{1}{C_2 - C_1}\int_{C_1}^{C_2}(p + qe^{-rC})\,\mathrm{d}C = \frac{1}{C_2 - C_1}\left[pC - \frac{q}{r}e^{-C}\right]_{C_1}^{C_2}$$
$$= 1 - \frac{q}{r}\frac{e^{-pC_1} - e^{-pC_2}}{C_2 - C_1} \tag{13}$$

The resulting effective area resistances are 5.90 Ω cm^2 for the FKD and 1.63 Ω cm^2 for the FAD if used NaCl concentrations of C_2 = 0.51 mol/L (=30 g/L) and C_1 = 0.017 mol/L (=1 g/L). For the used membranes it follows that the resulting resistance is about twice the resistances between solutions of 0.5 mol NaCl/L.

Nomenclature

A	cell area (m^2)
a, b, c	fit variables for P_{pump}
C	concentration (mol/m^3)
d, e	fit variables for P_{u}
E	voltage (V)
E_{cell}	electromotive force of one cell (V)
f	obstruction factor
F	Faraday constant (96,485 C/mol)
G_{RED}	free energy of the RED process (J)
I	electrical current (A)
J	electrical current density (A/m^2)
M	mol mass NaCl (0.0584 kg/mol)
N	number of cells in a stack
P_{d}	power density (W/m^2)
$P_{\text{d-net}}$	net power density (W/m^2)
P_{max}	maximum external power (W)
P_{u}	external power (W)
P_{pump}	hydrodynamic loss (W)
R_{AEM}	cation exchange membrane resistance (Ω)
R_{CEM}	cation exchange membrane resistance (Ω)
R_{area}	area resistance of a membrane (Ω m^2)
R_{eff}	effective area resistance of a membrane (Ω m^2)
R_{i}	internal resistance (Ω)
R_{u}	external resistance (Ω)
R_{river}	river water compartment resistance (Ω)
R_{sea}	sea water compartment resistance (Ω)
R^2	determination coefficient
R	gas constant (8.31432 J mol^{-1} K^{-1})
t_{w}	electro-osmotic water transport number (mol/F)
S	salt content (kg/m^3)
T	temperature (K)
OCV	open circuit voltage (V)
p, q, r	fit variables for R_{eff}
V	volume (m^3)
X_{in}	free energy per second of the inlet (W)

X_{out}	free energy per second of the effluent (W)
X_{cons}	consumed free energy per second (W)
X_{max}	maximal available free energy per second (W)
Y	energy efficiency
Y_{gross}	gross energy efficiency

Greek symbols

α	permselectivity of the ion exchange membrane
δ_C	compartment thickness (m)
δ_M	membrane thickness (m)
η_P	power efficiency
Φ	flow (m^3/s)

Superscripts

i	in
o	out

Subscripts

S	sea
R	river
M	equilibrium

Abbreviations

AEM	anion exchange membrane
CEM	cation exchange membrane
ED	electrodialysis
EMF	electromotive force (V)
RED	reverse electrodialysis

Definitions

compartment	space between the membranes
cell	combination of two membranes and two compartments
electrode system	the anode, cathode and electrode rinse
stack	a number of N cells with an electrode system

References

[1] R.E. Pattle, Production of electric power by mixing fresh and salt water in the hydroelectric pile, Nature 174 (1954) 660.
[2] G.L. Wick, W.R. Schmitt, Prospects for renewable energy from sea, Mar. Technol. Soc. J. 11 (1977) 16–21.
[3] Energy information administration; official energy statistics from the U.S. government. www.eia.doe.gov.
[4] R.E. Pattle, Electricity from fresh and salt water—without fuel, Chem. Proc. Eng. 35 (1955) 351–354.
[5] R.E. Pattle, Improvements to electric batteries, Patent GB731729 (1955).
[6] S. Loeb, Osmotic power plants, Science 189 (1975) 654–655.
[7] S. Loeb, Production of energy from concentrated brines by pressure retarded osmosis. 1. Preliminary technical and economic correlations, J. Membr. Sci. 1 (1976) 49–63.
[8] M. Olsson, G.L. Wick, J.D. Isaacs, Salinity gradient power—utilizing vapor–pressure differences, Science 206 (1979) 452–454.
[9] M.V. Sussman, A. Katchalsky, Mechanochemical turbine: a new power cycle, Science 167 (1970) 45–47.
[10] W. Finley, E. Pscheidt, Hydrocratic generator, US Patent 6,313,545 B1 (2001).
[11] G. Lagger, H. Jensen, J. Josserand, H.H. Girault, Hydro-voltaic cells. Part 1. Concentration cells, J. Electroanal. Chem. 5445 (2003) 1–6.
[12] V. Kniajev, Energy of salinity gradient—new source of energy with minimal environmental impact, in: Abstracts from the International Workshop "Result of Fundamental Research for Investments" (IWRFRI'2001'), St. Petersburg, Russia, 2001.
[13] J.W. Post, J. Veerman, H.V.M. Hamelers, G.J.W. Euverink, S.J. Metz, K. Nymeijer, C.J.N. Buisman, Salinity-gradient power: Evaluation of pressure-retarded osmosis and reverse electrodialysis, J. Membr. Sci. 288 (2007) 218–230.
[14] J.N. Weinstein, F.B. Leitz, Electric power from differences in salinity: the dialytic battery, Science 191 (1976) 557–559.
[15] R. Audinos, Inverse electrodialysis. Study of electric energy obtained starting with two solutions of different salinity, J. Power Sources 10 (1983) 203–217 (in French).
[16] R. Audinos, Electric power produced from two solutions of unequal salinity by reverse electrodialysis, Ind. J. Chem. 31A (1992) 348–354.
[17] J. Jagur-Grodzinski, R. Kramer, Novel process for direct conversion of free energy of mixing into electric power, Ind. Eng. Chem. Process Des. Dev. 25 (1986) 443–449.
[18] M. Turek, B. Bandura, Renewable energy by reverse electrodialysis, Desalination 205 (2007) 67–74.
[19] F. Suda, T. Matsuo, D. Ushioda, Transient changes in the power output from the concentration difference cell (dialytic battery) between seawater and river water, Energy 32 (2007) 165–173.
[20] J. Veerman, J.W. Post, S.J. Metz, M. Saakes, G.J. Harmsen, Reducing power losses caused by ionic shortcut currents in reverse electrodialysis stacks by a validated model, J. Membr. Sci. 310 (2008) 418–430.
[21] B.H. Clampitt, F.E. Kiviat, Energy recovery from saline water by means of electrochemical cells, Science 194 (1976) 719–720.
[22] R.E. Lacey, Energy by reverse electrodialysis, Ocean Eng. 7 (1980) 1–47.
[23] C. Forgacs, Generation of electricity by reverse electrodialysis, BGUN-RDA – 178-78, Ben-Gurion University, Israel, 1978.
[24] C. Forgacs, R.N. O'Brien, Utilization of membrane processes in the development of non-conventional renewable energy sources, Chem. Can. 31 (1979) 19–21.
[25] V.I. Zabolotsky, V.V. Nikonenko, Effect of structural membrane inhomogeneity on transport properties, J. Membr. Sci. 79 (1993) 181–189.
[26] L.X. Tuan, C. Buess-Herman, Study of water content and microheterogeneity of CMS cation exchange membrane, Chem. Phys. Lett. 434 (2007) 49–55.
[27] P. Długołęcki, K. Nymeijer, S. Metz, M. Wessling, Current status of ion exchange membranes for power geration from salinity gradients, J. Membr. Sci. 319 (2008) 214–222.
[28] M.H. Dirkse, W.K.P. van Loon, J.W. Post, J. Veerman, J.D. Stigter, G.P.A. Bot, Extending potential flow modelling of flat-sheet geometries as applied in membrane-based systems, J. Membr. Sci. 325 (2008) 537–545.